

Volume 71 (2015)

**Supporting information for article:**

**Synergy between transmission electron microscopy and powder diffraction: application to modulated structures**

**Dmitry Batuk, Maria Batuk, Artem M. Abakumov and Joke Hadermann**

**Table S1** Overview of the modulated structures refined from powder diffraction data.

Composition	Radiation	TEM data	Reference
$\alpha$ -PbO	laboratory XPD + NPD (extraction of intensities and refinement in single crystal mode)	none	Hédoux et al., 1989
$\text{Bi}_2\text{Sr}_{1.5}\text{Ca}_{1.5}\text{Cu}_2\text{O}_y$	simultaneous laboratory XPD + NPD	none	Yamamoto et al., 1990
$\text{Bi}_{2.2}\text{Sr}_{1.8}\text{CuO}_{6+y}$	simultaneous laboratory XPD + NPD	none	Yamamoto et al., 1992
$\text{Sr}_{1.19}\text{TiS}_3$	laboratory XPD	none	Onoda & Saeki, 1993
$\text{Sr}_{1.145}\text{TiS}_3$	laboratory XPD	SAED	Onoda et al., 1993
$\text{Bi}_{2.3}\text{Sr}_{1.7}\text{CuO}_{6.23}$ $\text{Bi}_2\text{Sr}_{1.7}\text{La}_{0.3}\text{CuO}_{6.28}$	laboratory XPD	none	Khasanova & Antipov, 1995
$\text{Ba}_{0.85}\text{Ca}_{2.15}\text{In}_6\text{O}_{12}$	simultaneous XPD (rotating anode) + NPD	SAED, HRTEM	Baldinozzi et al., 1996
$\text{Ca}_{13.6}\text{Sr}_{0.4}\text{Cu}_{24}\text{O}_{41}$	simultaneous laboratory XPD + NPD	SAED	Ohta et al., 1997
$\text{Pb}_2\text{MgTeO}_6$	NPD	none	Baldinozzi et al., 1998
$\text{Pb}_2\text{MgTe}_{0.6}\text{W}_{0.4}\text{O}_6$	NPD	none	Rivezzi & Sciau, 1998
$(\text{Ba}_{0.65}\text{Bi}_{0.35})(\text{Fe}_{0.9}\text{Bi}_{0.1})\text{O}_{2.675}$ $(\text{Ba}_{0.56}\text{Bi}_{0.44})(\text{Fe}_{0.96}\text{Bi}_{0.04})\text{O}_{2.72}$	laboratory XPD (rotating anode)	SAED, HRTEM	Boullay, Grebille et al., 1999
$(\text{Ba}_{0.56}\text{Bi}_{0.44})(\text{Fe}_{0.96}\text{Bi}_{0.04})\text{O}_{2.72}$	simultaneous laboratory XPD (rotating anode) + NPD		
$\text{Cu}_8\text{GeSe}_6$	SXPD	none	Onoda et al., 1999
$\text{Pb}_2\text{CoWO}_6$	NPD	SAED	Baldinozzi et al., 2000
$\text{Sr}_8\text{Ca}_6\text{Cu}_{24}\text{O}_{41}$ $\text{Sr}_{0.4}\text{Ca}_{13.6}\text{Cu}_{24}\text{O}_{41}$	SXPD	none	Bougerol-Chaillout et al., 2000
$\text{Sr}_{0.4}\text{Ca}_{13.6}\text{Cu}_{24}\text{O}_{41}$	NPD	SAED	Isobe et al., 2000
$\text{NbTe}_4$	laboratory XPD	none	Dušek et al., 2001
$\text{La}_5\text{Ti}_4\text{O}_{15}$	laboratory XPD	none	Petříček et al., 2001
$\text{BaLa}_4\text{Ti}_4\text{O}_{15}$	simultaneous laboratory XPD + NPD		
$\alpha$ -PbO	SXPD	none	Baldinozzi et al., 2002
$\text{Ca}_{0.83}\text{CuO}_2$	simultaneous laboratory XPD + NPD	none	Miyazaki, Onoda, Edwards et al., 2002
$[\text{Ca}_2\text{CoO}_3]_{0.62}\text{CoO}_2$	simultaneous laboratory XPD + NPD	SAED	Miyazaki, Onoda, Oku et al., 2002
$\text{Sr}_{1.32}\text{Mn}_{0.83}\text{Cu}_{0.17}\text{O}_3$	laboratory XPD	SAED, HRTEM	Abakumov et al., 2003

Composition	Radiation	TEM data	Reference
$\text{Ba}_6\text{TiNb}_4\text{O}_{18}$	laboratory XPD	none	Boullay et al., 2003
$\text{Ba}_{11}\text{TiNb}_8\text{O}_{33}$			
$\text{Sr}_{1.3244}\text{Mn}_{0.6756}\text{Cu}_{0.3244}\text{O}_3$	laboratory XPD	none	El Abed et al., 2003
SiO <sub>2</sub> -trydimite	laboratory XPD	none	Graetsch, 2003
Te(8.5 GPa)	SXPD	none	Hejny & McMahon, 2003
$\text{Ba}_2\text{TiGe}_2\text{O}_8$	NPD	none	Höche et al., 2003
$\text{Sr}_{1.27}(\text{Co}_{0.27}\text{Mn}_{0.73})\text{O}_3$	NPD	none	Jordan et al., 2003
Iodine(24.6 GPa)	SXPD	none	Kenichi et al., 2003
$[\text{Ca}_2(\text{Co}_{0.65}\text{Cu}_{0.35})_2\text{O}_4]_{0.63}\text{CoO}_2$	NPD	SAED	Miyazaki et al., 2003
MnTa <sub>2</sub> O <sub>6</sub>	laboratory XPD	SAED	Tarakina et al., 2003
Sb(6.9GPa)	SXPD	none	Degtyareva et al., 2004
SrMn <sub>3</sub> O <sub>6</sub>	NPD	SAED, HRTEM	Gillie et al., 2004
$[\text{Ca}_2\text{CoO}_3][\text{CoO}_2]_{1.62}$	NPD	none	Grebillie et al., 2004
$\text{Ca}_{0.82}(\text{Cu}_{0.65}\text{Co}_{0.35}\text{O}_2)$	NPD	none	
Ni <sub>1.35</sub> Sn			
Ni <sub>1.38</sub> Sn	laboratory XPD	none	Leineweber, 2004
Ni <sub>1.41</sub> Sn			
InCr <sub>0.33</sub> Ti <sub>0.67</sub> O <sub>3.33</sub>	laboratory XPD	none	Michiue et al., 2004
Sr <sub>1.14</sub> TiS <sub>2.84</sub>	laboratory XPD	none	Onoda & Saeki, 2004
Sc (23 GPa)	SXPD	none	Fujihisa et al., 2005
SiO <sub>2</sub> -trydimite(438 K)	SXPD	none	Graetsch & Brunelli, 2005
S(100.5 GPa)	SXPD	none	Hejny et al., 2005
In <sub>6</sub> Ti <sub>6</sub> CaO <sub>22</sub>	laboratory XPD	SAED	Li et al., 2005
Ga <sub>4</sub> Ti <sub>13</sub> O <sub>32</sub>	SXPD	none	Michiue et al., 2006
KNd(MoO <sub>4</sub> ) <sub>2</sub>	laboratory XPD	SAED, HRTEM	Morozov, Arakcheeva et al., 2006
$\text{Ag}_{1/8}\text{Pr}_{5/8}\text{MoO}_4$	laboratory XPD	SAED	Morozov, Mironov et al., 2006
La <sub>4</sub> O <sub>2</sub> F <sub>2</sub> S <sub>3</sub>	laboratory XPD	SAED	Pauwels et al., 2006
Ni <sub>2</sub> MnGa	laboratory XPD	none	Righi et al., 2006
Sr <sub>0.61</sub> Ba <sub>0.39</sub> Nb <sub>2</sub> O <sub>6</sub>	NPD	none	Schefer et al., 2006
LiB <sub>0.885</sub>	NPD	none	Wörle et al., 2006
$[\text{SrF}_{0.8}(\text{OH})_{0.2}]_{2.526}[\text{Mn}_6\text{O}_{12}]$	laboratory XPD	SAED, HRTEM	Abakumov et al., 2007
P(125 GPa)	SXPD	none	Fujihisa et al., 2007
AlPO <sub>4</sub>	laboratory XPD	none	Graetsch, 2007

Composition	Radiation	TEM data	Reference
LaSrCuO <sub>3.52</sub>	NPD	SAED, HRTEM	Hadermann et al., 2007
(Ca <sub>0.85</sub> OH) <sub>1.156</sub> CoO <sub>2</sub>	SXPD	SAED	Isobe et al., 2007
NiGe <sub>1-x</sub> P <sub>x</sub> , x = 0.4, 0.5, 0.6, 0.7	laboratory XPD	none	Larsson, García-García et al., 2007
Ni <sub>3</sub> InTe <sub>2</sub>	NPD	none	Larsson, Noren et al., 2007
Sr <sub>1.31</sub> Co <sub>0.63</sub> Mn <sub>0.37</sub> O <sub>3</sub>	NPD	SAED, HAADF- STEM	Mandal et al., 2007
Ni <sub>1.95</sub> Mn <sub>1.19</sub> Ga <sub>0.86</sub>	laboratory XPD	none	Righi et al., 2007
Na <sub>1.58</sub> CuO <sub>2</sub> Na <sub>1.62</sub> CuO <sub>2</sub>	SXPD	none	van Smaalen et al., 2007
Ba <sub>4</sub> In <sub>6</sub> O <sub>12.99</sub> Ba <sub>4</sub> In <sub>5.6</sub> Mg <sub>0.4</sub> O <sub>12.8</sub>	laboratory XPD	SAED, HRTEM	Abakumov, Rossell et al., 2008
KSm(MoO <sub>4</sub> ) <sub>2</sub>	SXPD	SAED, HRTEM	Arakcheeva et al., 2008
Thiophene	NPD	none	Damay et al., 2008
ErFe <sub>6</sub> Ge <sub>3</sub> Ga <sub>3</sub>	laboratory XPD	none	Fredrickson et al., 2008
MnSi <sub>1.74</sub>	NPD	none	Miyazaki et al., 2008
Ni <sub>2</sub> Mn <sub>1.2</sub> Ga <sub>0.8</sub>	laboratory XPD	none	Righi et al., 2008
Bi <sub>2</sub> Mn <sub>4/3</sub> Ni <sub>2/3</sub> O <sub>6</sub>	NPD	SAED	Claridge et al., 2009
Ni <sub>1.6</sub> Sn	laboratory XPD	none	Leineweber, 2009
CaMn <sub>7</sub> O <sub>12</sub>	SXPD	none	Sławiński et al., 2009
Sr <sub>1.261</sub> CoO <sub>3</sub>	NPD	none	Isobe et al., 2010
LiZnNb <sub>4</sub> O <sub>11.5</sub>	SXPD	SAED, HRTEM	Morozov et al., 2010
Ni <sub>2.41</sub> Fe <sub>0.59</sub> Ga	NPD	none	Righi et al., 2010
Pb <sub>0.64</sub> Bi <sub>0.32</sub> Fe <sub>1.04</sub> O <sub>2.675</sub> (700 K)	NPD	SAED, HAADF- STEM	Abakumov et al., 2011
Sr <sub>14-x</sub> Ca <sub>x</sub> Cu <sub>24</sub> O <sub>41</sub> , x = 3, 7, 11, 12.2	NPD	none	Deng et al., 2011
Bi <sub>0.75</sub> La <sub>0.25</sub> FeO <sub>3</sub>	SXPD	SAED, HRTEM	Rusakov et al., 2011
Na <sub>x</sub> Eu <sub>(2-x)/3</sub> MoO <sub>4</sub> , x = 0.25, 0.236, 0.2, 0.138, 0.134, 0.015	SXPD	none	Arakcheeva et al., 2012
Bi <sub>2(n+2)</sub> Mo <sub>n</sub> O <sub>6(n+1)</sub> , n = 3, 4, 5, 6	simultaneous SXRD + NPD	none	Bereciartua et al., 2012

Composition	Radiation	TEM data	Reference
Eu-34GPa	SXPD	none	Husband et al., 2012
(1-x)Ta <sub>2</sub> O <sub>5</sub> xAl <sub>2</sub> O <sub>3</sub> , x = 0, 0.04, 0.05, 0.07, 0.08	SXPD	none	Schmid & Fung, 2012
Li <sub>0.15</sub> Nd <sub>0.617</sub> TiO <sub>3</sub>	simultaneous SXRD + NPD	SAED, HAADF-STEM	Abakumov et al., 2013
Pb <sub>0.792</sub> Sr <sub>0.168</sub> Fe <sub>1.040</sub> O <sub>2.529</sub> (900 K)	NPD	SAED, HAADF-STEM	Batuk, Batuk, Abakumov et al., 2013
Bi <sub>5</sub> Nb <sub>3</sub> O <sub>15</sub>	laboratory XPD	PED	Boullay et al., 2013
CuV <sub>2</sub> S <sub>4</sub>	SXPD	none	Kawaguchi et al., 2013
Ni <sub>2</sub> MnGa	SXPD	none	Singh et al., 2013
CaEu <sub>2</sub> (WO <sub>4</sub> ) <sub>4</sub> CaEu <sub>2</sub> (MoO <sub>4</sub> ) <sub>4</sub>	SXPD	SAED, HAADF-STEM	Abakumov et al., 2014
PdB <sub>0.184</sub>	NPD	SAED	Leineweber et al., 2014
Ni <sub>2</sub> MnGa	SXPD	none	Singh et al., 2014

XPD – X-ray powder diffraction

SXPD – synchrotron X-ray powder diffraction

NPD – neutron powder diffraction

SAED – selected area electron diffraction

PED – precession electron diffraction

HRTEM – high resolution transmission electron microscopy

HAADF-STEM – high angle annular dark field scanning transmission electron microscopy

## S1 Crystal structure refinement of the $(\text{Pb},\text{Bi})_{1-x}\text{Fe}_{1+x}\text{O}_{3-y}$ compounds

To analyze exact atomic displacement modulations in the  $(\text{Pb},\text{Bi})_{1-x}\text{Fe}_{1+x}\text{O}_{3-y}$  system and their evolution upon the variation of thickness of the perovskite blocks (i.e. anion content defined by the  $\text{Pb}^{2+}/\text{Bi}^{3+}$  ratio), we have refined the crystal structure of 5 compounds with different Bi concentration in the A positions (10, 20, 30, 44 and 56 at.%) that cover the entire existence range of the  $(\text{Pb},\text{Bi})_{1-x}\text{Fe}_{1+x}\text{O}_{3-y}$  series. Since both cationic and anionic sublattices in the structures are subjected to strong atomic displacements, neutron powder diffraction (NPD) data were chosen for the refinement. The neutron scattering length of O (5.803 fm) is comparable to that of Fe (9.450 fm), Pb (9.405 fm) and Bi (8.532 fm) (Sears, 1992); and therefore unlike X-ray powder diffraction allows accurate refinement of displacive modulations of light oxygen atoms in the presence of Pb and Bi. All the investigated materials in the  $(\text{Pb},\text{Bi})_{1-x}\text{Fe}_{1+x}\text{O}_{3-y}$  series are antiferromagnetically ordered below  $T_N \approx 600$  K. To eliminate the contribution of the magnetic scattering, the NPD data collected at 900 K were used for the refinement.

As an initial model for the Rietveld refinement, we used the occupational superspace model describing the atomic arrangement of the structures (see the main text and Abakumov et al., 2011). Parameters of the occupational model in the general case and numerical values for each compound are listed in Table S3. All the atomic domains in this model are defined on intervals along  $x_4$  shorter than 1. In this case, refinement of the atomic displacement modulations using harmonic functions is not possible, because the components of the truncated Fourier series are not orthogonal on the interval shorter than 1, which results in correlations between the modulation components. To avoid this problem, displacive modulations were refined in the form of Legendre polynomials (Dušek et al., 2010). This way, displacive modulation of an atom v is given as:

$$\mathbf{U}^v = \sum_n \left\{ \mathbf{S}_{(2n-1)}^v P_{(2n-1)} [2(\bar{x}_4 - x_4^0)/\Delta] + \mathbf{S}_{(2n)}^v P_{(2n)} [2(\bar{x}_4 - x_4^0)/\Delta] \right\},$$

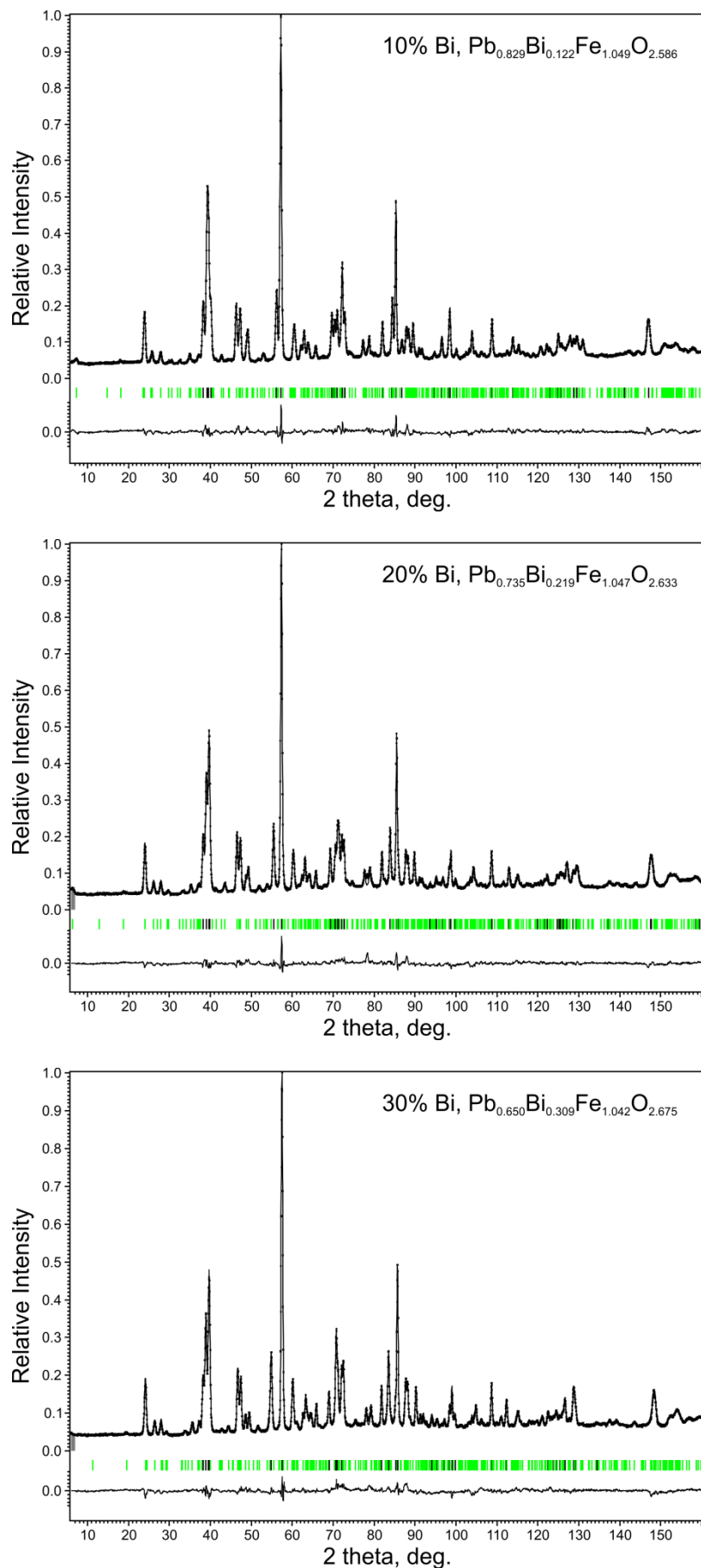
where  $P_i(x) = [1/2^i i!] (d^i/dx^i) [(x^2 - 1)^i]$  are Legendre polynomials, n is the order of the modulation wave and  $\mathbf{S}_n$  are the coefficients of the series expansion. Polynomials of two orders are required to describe one order of the modulation wave; i.e.,  $P_1$  and  $P_2$  form the first modulation wave,  $P_3$  and  $P_4$  the second wave, etc. The  $P_1$  component defines linear displacements of the atoms, and the coefficients  $\mathbf{S}_1$  represent maximal linear displacements of the atom. The  $X2/m(a0\gamma)00$  [ $X = (1/2, 1/2, 1/2, 1/2)$ ] symmetry rules out all even components, so that  $\mathbf{S}_{2n} = 0$  and  $\mathbf{U}^v = \sum_n \left\{ \mathbf{S}_{(2n-1)}^v P_{(2n-1)} [2(\bar{x}_4 - x_4^0)/\Delta] \right\}$ .

The results of the Rietveld refinement of the structures with 10, 20, 30, 44 and 56 at.% Bi in the A positions are represented in Fig. S1 and Tables S2-S4.

Refinement of the atomic displacive modulations revealed that for all compounds a satisfactory fit of the experimental data is achieved, when the modulation waves up to second order are used for each atomic position. Introduction of higher orders modulations insignificantly improved the fit, yet resulted in uneven behavior the modulation functions leading to unreasonably long and short Fe-O distances close to and at the CS planes, respectively. Besides, in structures with narrow perovskite blocks (10, 20 and 30 at.% Bi), it was even found that some coefficients of the second order components ( $\mathbf{S}_{z,3}$  for O2 and  $\mathbf{S}_{x,3}$  for O3) are smaller

than their standard deviations. These parameters were fixed to zeros, which did not affect the fit. Noticeable improvement of the R factors was achieved refining anisotropic atomic displacement parameters (ADPs) for the O1 positions. In all the structures they exhibit large  $U_{11}$  and  $U_{33}$  components, while the  $U_{22}$  is considerably smaller. This can be explained by inherent defects present at the CS planes, where local violations of translational symmetry along the  $b$  direction locally transform chains of quadruple edge-sharing  $\text{FeO}_5$  pyramids into double edge-sharing  $\text{FeO}_5$  pyramidal chains (see Fig. S2). This affects the O1 atomic positions most, because they create the edges shared by the  $\text{FeO}_5$  pyramids. Although such defects intermix the Fe and (Pb,Bi) positions, they practically do not affect their modulations, because the CS planes interrelate these positions in the adjacent perovskite blocks (i.e.  $\Delta[\text{Fe}] + \Delta[\text{Pb,Bi}] = 1$ , but  $x_4^0[\text{Fe}] = 0$  and  $x_4^0[\text{Pb,Bi}] = 0.5$ ) and the neutron scattering lengths for Pb, Bi and Fe are very similar.

Analyzing coefficients of the atomic displacive modulation waves (Table S4) one can notice that their values for different structures are quite similar. It results in a very similar coordination of the Fe and (Pb,Bi) positions (Fig. S3 and Fig. 8 in the main text). Therefore, it can be assumed that the anion deficient perovskites in the  $(\text{Pb,Bi})_{1-x}\text{Fe}_{1+x}\text{O}_{3-y}$  family not only share the same building principles but also demonstrate a very similar distortion patterns of the perovskite blocks, that are caused by the periodic arrangement of the CS planes. The most noticeable systematic changes of the  $(\text{Pb,Bi})_{1-x}\text{Fe}_{1+x}\text{O}_{3-y}$  structures upon variation of the Bi content are associated with the modulation of the (Pb,Bi) positions (see the corresponding  $S_1$  and  $S_3$  parameters in Table S4). It can be attributed to the increasing flexibility of the perovskite blocks with the increasing thickness, so that the rows of the (Pb,Bi) atomic columns acquire pronounced wave-like shape along the  $a$  direction (see structure images in Fig. 7 and HAADF-STEM images in Figs. 4 and 10 of the main text). Nevertheless, in all structures the (Pb,Bi)-O distances and the cubooctahedral distortion parameters (introduced to parametrize the distortion of the (Pb,Bi) coordination environment, see the main text) demonstrate the same changes upon going from the center of the perovskite blocks towards the CS planes. The distortions of the  $\text{FeO}_6$  cubooctahedra close to the CS planes, systematically decrease with increasing thickness of the perovskite blocks:  $\Delta_{\text{oct}}^{\max}[20\%\text{Bi}] = 2.55 \cdot 10^{-2}$ ;  $\Delta_{\text{oct}}^{\max}[30\%\text{Bi}] = 2.36 \cdot 10^{-2}$ ;  $\Delta_{\text{oct}}^{\max}[44\%\text{Bi}] = 2.23 \cdot 10^{-2}$ ;  $\Delta_{\text{oct}}^{\max}[56\%\text{Bi}] = 2.04 \cdot 10^{-2}$ . The only exception is the compound with 10 at.% of Bi ( $\Delta_{\text{oct}}^{\max}[10\%\text{Bi}] = 1.93 \cdot 10^{-2}$ ), which can be attributed to the presence of mirror twinning defects, fragmenting some crystals into very small domains (see Fig. S4). This affects the powder diffraction data and hence the crystal structure refinement.



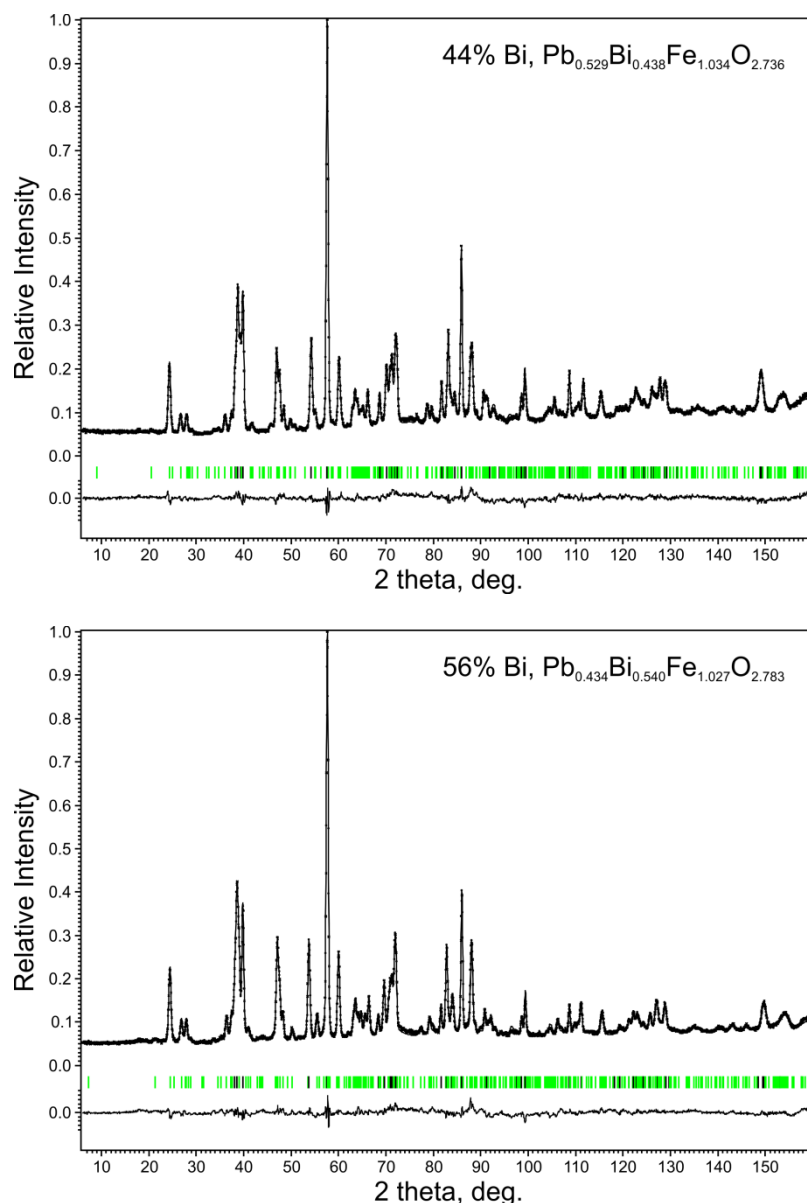


**Figure S1** Experimental, calculated and difference NDP profiles ( $\lambda = 1.8857 \text{\AA}$ ,  $T = 900 \text{ K}$ ) for 5 compounds in the  $(\text{Pb,Bi})_{1-x}\text{Fe}_{1+x}\text{O}_{3-y}$  family after the Rietveld refinement. Black and green vertical lines indicated positions of the main and satellite reflections, respectively.

**Table S2** Selected crystallographic data and some parameters of Rietveld refinement for the compounds of the  $(\text{Pb},\text{Bi})_{1-x}\text{Fe}_{1+x}\text{O}_{3-y}$  family

at.% of Bi in the A position <sup>a</sup>	10 at.%	20 at.%	30 at.%	44 at.%	56 at.%
Formula <sup>b</sup>	$\text{Pb}_{0.829}\text{Bi}_{0.122}\text{Fe}_{1.049}\text{O}_{2.586}$	$\text{Pb}_{0.735}\text{Bi}_{0.219}\text{Fe}_{1.047}\text{O}_{2.633}$	$\text{Pb}_{0.650}\text{Bi}_{0.309}\text{Fe}_{1.042}\text{O}_{2.675}$	$\text{Pb}_{0.529}\text{Bi}_{0.438}\text{Fe}_{1.034}\text{O}_{2.736}$	$\text{Pb}_{0.434}\text{Bi}_{0.540}\text{Fe}_{1.027}\text{O}_{2.783}$
Space Group	$X2/m(\alpha 0\gamma)$ , $X = [1/2, 1/2, 1/2, 1/2]$				
<i>a</i> , Å	3.9349(1)	3.9282(1)	3.9213(1)	3.9146(1)	3.9091(2)
<i>b</i> , Å	3.9319(1)	3.9266(1)	3.9195(1)	3.9127(1)	3.9059(1)
<i>c</i> , Å	4.0017(1)	4.0520(1)	4.0926(1)	4.1378(2)	4.1656(2)
$\beta$ , deg.	92.603(3)	92.209(3)	91.913(1)	91.554(3)	91.318(3)
$\alpha$	0.0667(2)	0.0570(2)	0.0500(1)	0.0410(2)	0.0342(1)
$\gamma$	0.1159(1)	0.1035(1)	0.0916(1)	0.0745(1)	0.0609(2)
<i>h/l = a/γ</i> <sup>c</sup>	0.575	0.551	0.546	0.550	0.562
Calculated density, g/cm <sup>3</sup>	7.989(9)	7.958(8)	7.951(6)	7.946(6)	7.953(5)
T, K			900		
Radiation			Neutrons, $\lambda = 1.8857\text{\AA}$		
2θ range, deg.; step 0.05	$6 \leq 2\theta \leq 160$	$7 \leq 2\theta \leq 160$	$7 \leq 2\theta \leq 160$	$6 \leq 2\theta \leq 160$	$6 \leq 2\theta \leq 160$
$R_F$ (all reflections)	0.039	0.040	0.049	0.052	0.055
$R_F$ (main reflections)	0.022	0.028	0.035	0.033	0.028
$R_F$ (1 <sup>st</sup> order satellites)	0.042	0.042	0.048	0.048	0.053
$R_F$ (2 <sup>nd</sup> order satellites)	0.052	0.050	0.059	0.062	0.071
$R_F$ (3 <sup>d</sup> order satellites)	0.056	0.053	0.065	0.077	0.080
$R_F$ (4 <sup>th</sup> order satellites)	0.0543	0.045	0.075	0.078	0.075
$R_P$ , $R_{WP}$	0.039, 0.050	0.036, 0.046	0.038, 0.047	0.036, 0.045	0.039, 0.050

<sup>a</sup> The Bi/(Pb+Bi) ratio used for preparing single phase samples

<sup>b</sup> The composition of the compounds is given with respect to the occupational superspace model according to the formula  $\text{Pb}_{6\gamma+2\alpha}\text{Bi}_{1-7\gamma-\alpha}\text{Fe}_{1+\gamma-\alpha}\text{O}_{3-3\gamma-\alpha}$ . As it has been demonstrated in the initial report it fits the experimentally determined composition. Small variations are most probably associated with the presence of defects.

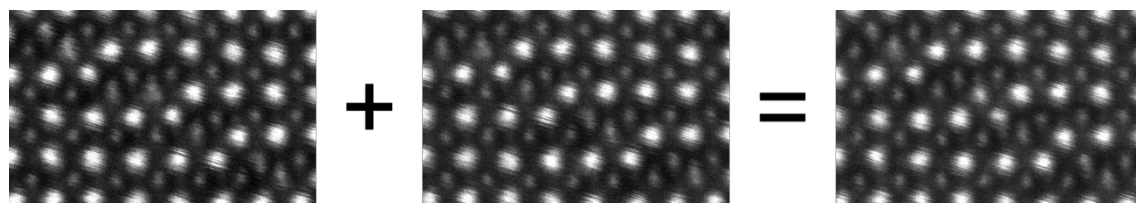
**Table S3** Parameters of the superspace occupational model for the refined structures in the  $(\text{Pb},\text{Bi})_{1-x}\text{Fe}_{1+x}\text{O}_{3-y}$  family.

atom	$x, y, z$	$x_4^0$	$\Delta$
$(1 - \alpha + \gamma)/2$			
Fe	0, 0, 0	0	10% Bi, $\text{Pb}_{0.829}\text{Bi}_{0.122}\text{Fe}_{1.049}\text{O}_{2.586}$ 0.5247
			20% Bi, $\text{Pb}_{0.735}\text{Bi}_{0.219}\text{Fe}_{1.047}\text{O}_{2.633}$ 0.5232
			30% Bi, $\text{Pb}_{0.650}\text{Bi}_{0.309}\text{Fe}_{1.042}\text{O}_{2.675}$ 0.5208
			44% Bi, $\text{Pb}_{0.529}\text{Bi}_{0.438}\text{Fe}_{1.034}\text{O}_{2.736}$ 0.5168
			56% Bi, $\text{Pb}_{0.434}\text{Bi}_{0.540}\text{Fe}_{1.027}\text{O}_{2.783}$ 0.5133
$(1 + \alpha - \gamma)/2$			
$(\text{Pb},\text{Bi})$	0, 0, 0	1/2	10% Bi, $\text{Pb}_{0.829}\text{Bi}_{0.122}\text{Fe}_{1.049}\text{O}_{2.586}$ 0.4753
			20% Bi, $\text{Pb}_{0.735}\text{Bi}_{0.219}\text{Fe}_{1.047}\text{O}_{2.633}$ 0.4767
			30% Bi, $\text{Pb}_{0.650}\text{Bi}_{0.309}\text{Fe}_{1.042}\text{O}_{2.675}$ 0.4792
			44% Bi, $\text{Pb}_{0.529}\text{Bi}_{0.438}\text{Fe}_{1.034}\text{O}_{2.736}$ 0.4832
			56% Bi, $\text{Pb}_{0.434}\text{Bi}_{0.540}\text{Fe}_{1.027}\text{O}_{2.783}$ 0.4867
$(1 - \alpha + \gamma)/2$			
O1	0, 1/2, 0	0	10% Bi, $\text{Pb}_{0.829}\text{Bi}_{0.122}\text{Fe}_{1.049}\text{O}_{2.586}$ 0.5247
			20% Bi, $\text{Pb}_{0.735}\text{Bi}_{0.219}\text{Fe}_{1.047}\text{O}_{2.633}$ 0.5232
			30% Bi, $\text{Pb}_{0.650}\text{Bi}_{0.309}\text{Fe}_{1.042}\text{O}_{2.675}$ 0.5208
			44% Bi, $\text{Pb}_{0.529}\text{Bi}_{0.438}\text{Fe}_{1.034}\text{O}_{2.736}$ 0.5168
			56% Bi, $\text{Pb}_{0.434}\text{Bi}_{0.540}\text{Fe}_{1.027}\text{O}_{2.783}$ 0.5133
$(1 + \alpha - 3\gamma)/2$			
O2	1/2, 0, 0	0	10% Bi, $\text{Pb}_{0.829}\text{Bi}_{0.122}\text{Fe}_{1.049}\text{O}_{2.586}$ 0.3594
			20% Bi, $\text{Pb}_{0.735}\text{Bi}_{0.219}\text{Fe}_{1.047}\text{O}_{2.633}$ 0.3733
			30% Bi, $\text{Pb}_{0.650}\text{Bi}_{0.309}\text{Fe}_{1.042}\text{O}_{2.675}$ 0.3876
			44% Bi, $\text{Pb}_{0.529}\text{Bi}_{0.438}\text{Fe}_{1.034}\text{O}_{2.736}$ 0.4088
			56% Bi, $\text{Pb}_{0.434}\text{Bi}_{0.540}\text{Fe}_{1.027}\text{O}_{2.783}$ 0.4258
$(1 - \alpha - \gamma)/2$			
O3	0, 0, 1/2	0	10% Bi, $\text{Pb}_{0.829}\text{Bi}_{0.122}\text{Fe}_{1.049}\text{O}_{2.586}$ 0.4087
			20% Bi, $\text{Pb}_{0.735}\text{Bi}_{0.219}\text{Fe}_{1.047}\text{O}_{2.633}$ 0.4198
			30% Bi, $\text{Pb}_{0.650}\text{Bi}_{0.309}\text{Fe}_{1.042}\text{O}_{2.675}$ 0.4292
			44% Bi, $\text{Pb}_{0.529}\text{Bi}_{0.438}\text{Fe}_{1.034}\text{O}_{2.736}$ 0.4423
			56% Bi, $\text{Pb}_{0.434}\text{Bi}_{0.540}\text{Fe}_{1.027}\text{O}_{2.783}$ 0.4525

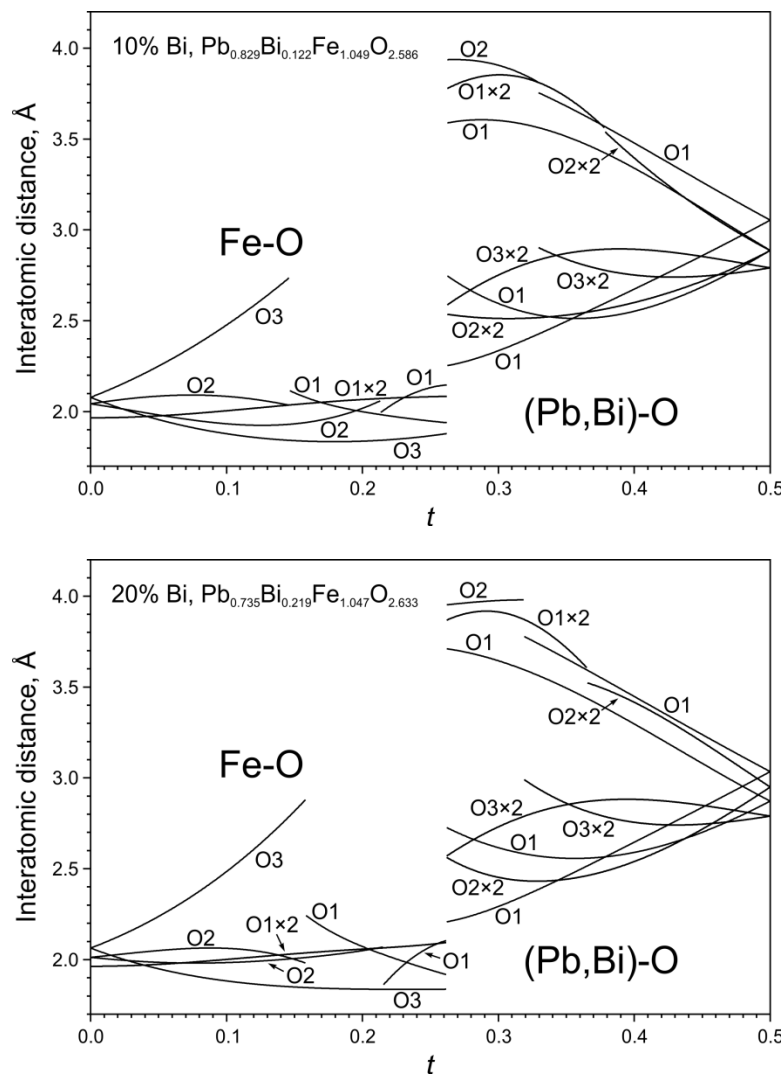
**Table S4** Modulation parameters of atomic displacements and ADP parameters for atomic positions in the refined structures in the  $(\text{Pb},\text{Bi})_{1-x}\text{Fe}_{1+x}\text{O}_{3-y}$  family.

atom	parameter	$\text{Pb}_{0.829}\text{Bi}_{0.122}\text{Fe}_{1.049}\text{O}_{2.586}$	$\text{Pb}_{0.735}\text{Bi}_{0.219}\text{Fe}_{1.047}\text{O}_{2.633}$	$\text{Pb}_{0.650}\text{Bi}_{0.309}\text{Fe}_{1.042}\text{O}_{2.675}$	$\text{Pb}_{0.529}\text{Bi}_{0.438}\text{Fe}_{1.034}\text{O}_{2.736}$	$\text{Pb}_{0.434}\text{Bi}_{0.540}\text{Fe}_{1.027}\text{O}_{2.783}$
Fe	$S_{x,1}$	0.030(1)	0.030(1)	0.027(1)	0.042(2)	0.057(2)
	$S_{z,1}$	0.058(1)	0.050(1)	0.042(1)	0.022(1)	0.016(1)
	$S_{x,3}$	-0.025(3)	-0.024(3)	-0.046(3)	-0.054(3)	-0.066(4)
	$S_{z,3}$	0.090(3)	0.105(3)	0.097(2)	0.097(3)	0.114(3)
	$U_{\text{iso}}$	0.0174(5)	0.0177(4)	0.0158(4)	0.096(4)	0.0202(6)
$(\text{Pb},\text{Bi})$	$g(\text{Bi})$	0.1	0.2	0.3	0.44	0.56
	$S_{x,1}$	0.007(1)	0.004(1)	0.010(2)	0.023(3)	0.047(3)
	$S_{z,1}$	-0.029(2)	-0.045(2)	-0.057(2)	-0.081(2)	-0.085(2)
	$S_{x,3}$	-0.078(5)	-0.085(5)	-0.091(6))	-0.102(5)	-0.093(5)
	$S_{z,3}$	0.094(4)	0.096(5)	0.104(5)	0.126(4)	0.156(5)
	$U_{\text{iso}}$	0.0537(9)	0.052(1)	0.053(1)	0.044(1)	0.056(1)
O1	$S_{x,1}$	0.033(5)	0.028(4)	0.037(4)	0.044(4)	0.056(3)
	$S_{z,1}$	0.266(3)	0.248(3)	0.235(3)	0.227(3)	0.208(2)
	$S_{x,3}$	-0.070(10)	-0.100(11)	-0.101(9)	-0.117(9)	-0.115(9)
	$S_{z,3}$	0.049(6)	0.069(5)	0.060(5)	0.083(5)	0.061(5)
	$U_{\text{eq}}$	0.039(2)	0.046(2)	0.038(2)	0.025(2)	0.033(1)
	$U_{11}$	0.065(3)	0.061(4)	0.058(4)	0.040(4)	0.056(3)
	$U_{22}$	0.003(1)	0.008(1)	0.007(1)	0.005(1)	0.012(2)
	$U_{33}$	0.050(4)	0.068(4)	0.049(3)	0.028(3)	0.028(4)
	$U_{12}$	0	0	0	0	0
	$U_{13}$	0.006(2)	0 *	-0.007(2)	-0.019(2)	-0.029(3)
O2	$U_{23}$	0	0	0	0	0
	$S_{x,1}$	0.055(7)	0.039(6)	0.044(5)	0.056(5)	0.062(5)
	$S_{z,1}$	0.138(4)	0.157(3)	0.142(2)	0.133(3)	0.105(4)
	$S_{x,3}$	-0.037(15)	-0.031(10)	-0.021(8)	-0.037(12)	-0.050(12)
	$S_{z,3}$	0.040(14)	0 *	0 *	0.041(11)	0.098(10)
O3	$U_{\text{iso}}$	0.046(2)	0.040(1)	0.044(1)	0.045(2)	0.063(1)
	$S_{x,1}$	0.024(3)	0.034(3)	0.049(2)	0.053(3)	0.056(3)
	$S_{z,1}$	0.132(3)	0.134(3)	0.129(2)	0.114(2)	0.098(2)
	$S_{x,3}$	0 *	0 *	0 *	-0.037(10)	-0.047(10)
	$S_{z,3}$	0.048(9)	0.071(7)	0.066(8)	0.065(8)	0.077(8)
	$U_{\text{iso}}$	0.049(1)	0.049(1)	0.047(1)	0.050(1)	0.065(1)

\* The refined values of these were smaller than their standard deviation and therefore they were fixed to 0.



**Figure S2** Schematic illustration of the “inherent” defects of the CS structures: local violations of the translational symmetry along the  $b$  direction. Bright dots correspond to the (Pb,Bi) atomic columns and faint dot – to the Fe-O columns.



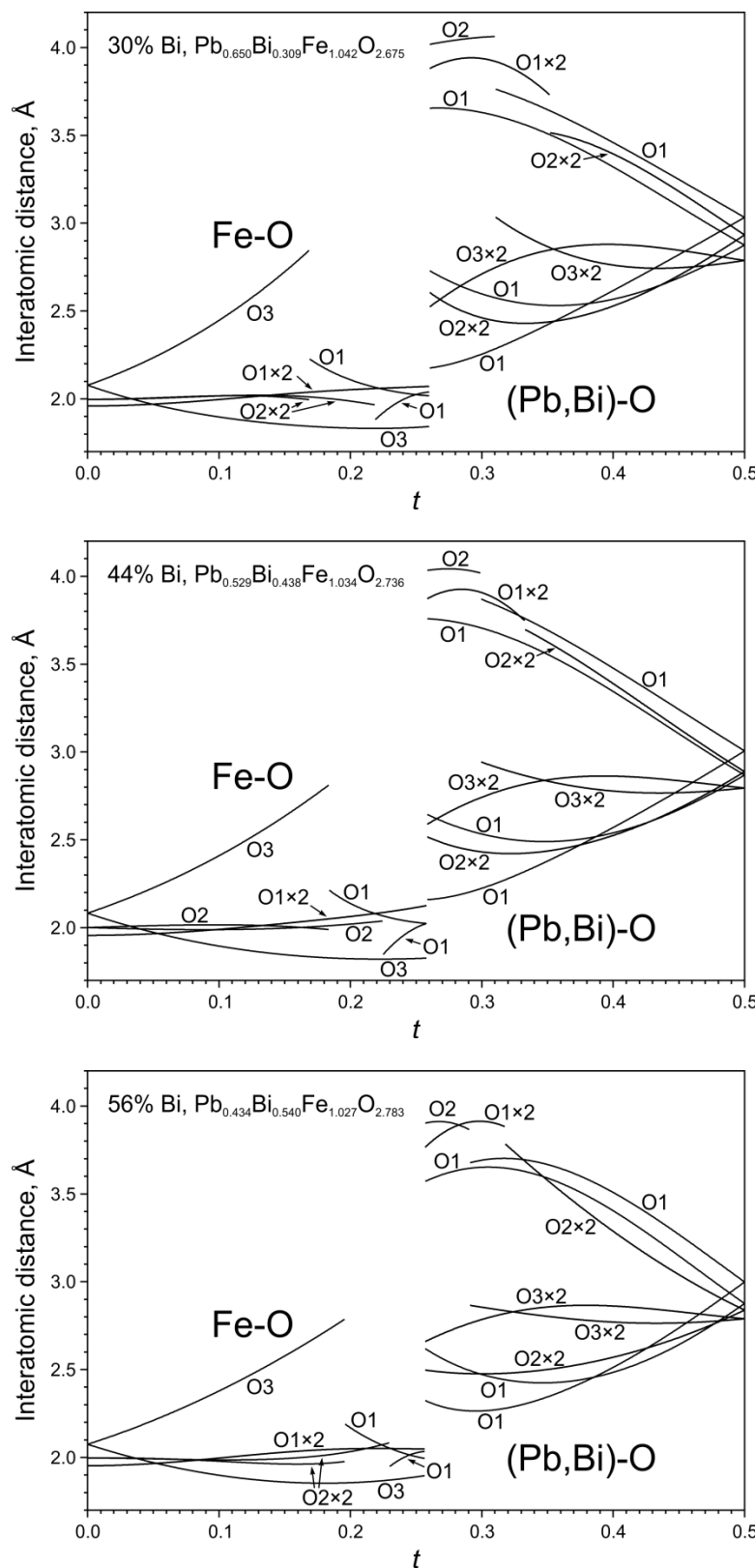


**Figure S3**  $t$ -plots of the Fe-O and (Pb,Bi)-O interatomic distances in the refined  $(\text{Pb},\text{Bi})_{1-x}\text{Fe}_{1+x}\text{O}_{3-y}$  structures. The curves for symmetry related O atoms are marked identically.

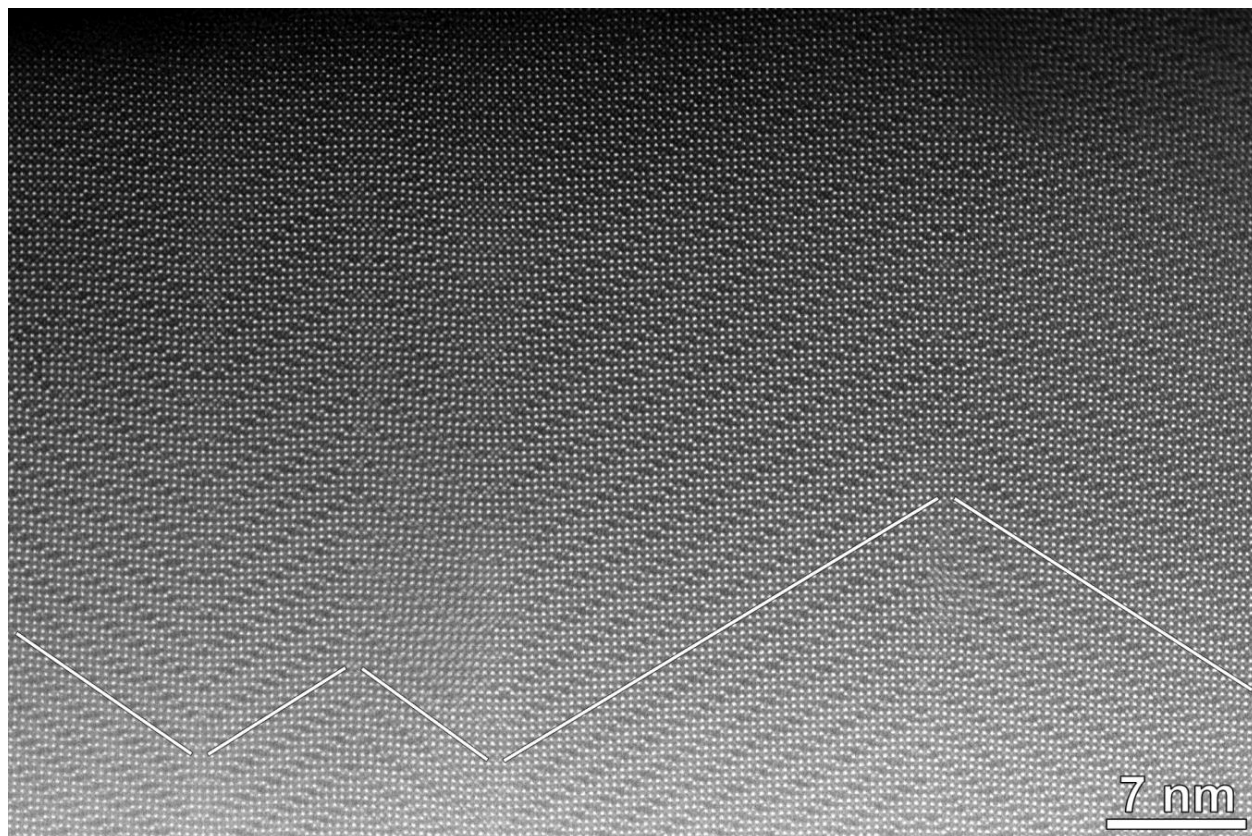


**Figure S4** HAADF-STEM image of the  $\text{Pb}_{0.829}\text{Bi}_{0.122}\text{Fe}_{1.049}\text{O}_{2.586}$  (10% Bi) material showing twinning in the structure, the most frequent type of defects in the  $(\text{Pb},\text{Bi})_{1-x}\text{Fe}_{1+x}\text{O}_{3-y}$  compounds with relatively low Bi concentrations. Lines highlight the orientation of the CS planes in the twinned domains.

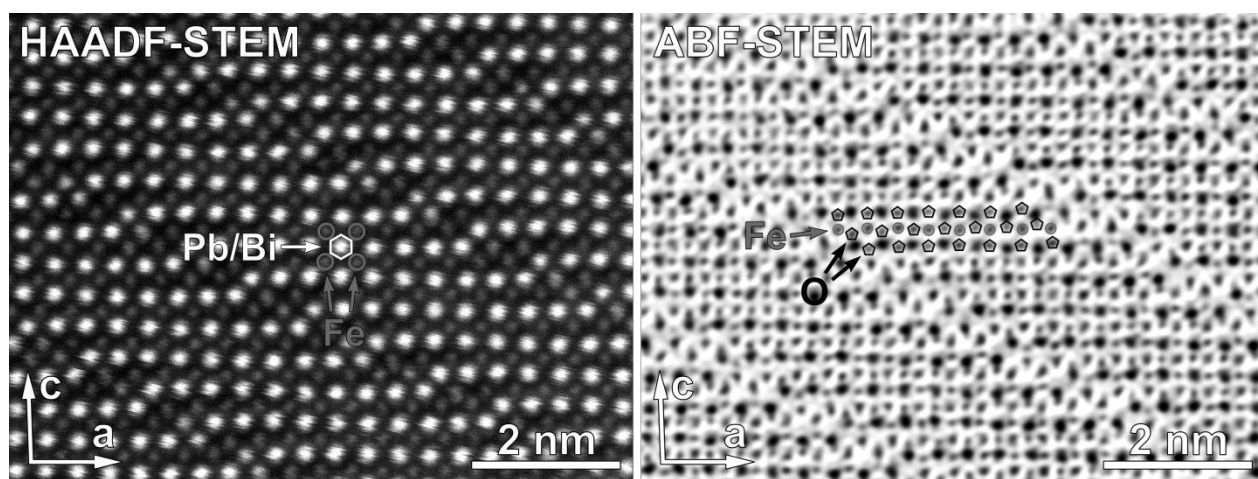


**Figure S5** Complimentary HAADF-STEM and ABF-STEM images of the  $\text{Pb}_{0.650}\text{Bi}_{0.309}\text{Fe}_{1.042}\text{O}_{2.675}$  compound, with indication of (Pb,Bi), Fe-O and O atomic columns.